

Spin-orbit-coupled superconductivity with spin-singlet non-unitary pairing

Meng Zeng,¹ Dong-Hui Xu,² Zi-Ming Wang,² and Lun-Hui Hu^{3,*}

¹*Department of Physics, University of California, San Diego, California 92093, USA*

²*Department of Physics, Hubei University, Wuhan 430062, China*

³*Department of Physics, the Pennsylvania State University, University Park, PA, 16802, USA*

An unconventional superconductor is distinguished with two types of gap functions: unitary and non-unitary. This core subject has been concentrated on purely spin-triplet or singlet-triplet mixed superconductors. However, the generalization to a purely spin-singlet superconductor has remained primarily of theoretical interest, which requires at least a multi-orbital correlated electronic systems. In this work, we present a possible establishment of both unitary and non-unitary pairings for spin-singlet superconductors with two atomic orbitals. Then we investigate the effects of atomic spin-orbit coupling and find a new spin-orbit-coupled non-unitary superconductor that supports exotic phenomena. Remarkably, there are mainly three features. Firstly, the atomic spin-orbit coupling locks the electron spins to be out-of-plane, which could give birth to the Type II Ising superconductivity with a large in-plane upper critical field compared to the Pauli limit. Secondly, topological chiral or helical Majorana edge state could be realized even in the absence of external magnetic fields or Zeeman fields. In addition, a spin-polarized superconducting state could even be generated by spin-singlet non-unitary pairings with spontaneous time-reversal breaking, which serves as a smoking gun to detect this exotic state by measuring the spin-resolved density of states. Therefore, our work might pave a new avenue to spin-orbit-coupled superconductors with spin-singlet non-unitary pairing symmetries.

I. INTRODUCTION

In condensed matter physics, research on unconventional superconductivity [1, 2] remains an crucial topic and continues to uncover new questions and challenges, since the discovery of the heavy-fermion superconductors (SCs) [3] and the d -wave pairing states in high-temperature cuprate SCs [4–7]. In addition to the anisotropic gap functions (e.g., p , d , f , g -wave...), the sublattice or orbital-dependent pairings [8–10] are alternative avenue to realize unconventional SCs. They might be realized in multi-orbital correlated electronic systems, whose candidate materials include iron-based SCs [11–21], Cu-doped Bi_2Se_3 [22, 23], half-Heusler compounds [24–33], and possibly Sr_2RuO_4 [34–37] etc. In particular, taking the atomic orbital degrees of freedom into account, the classification of unconventional pairing states could be significantly enriched. Among them, SCs with spontaneous time-reversal symmetry (TRS) breaking are of special interest, in which two mutually exclusive quantum phenomena, magnetism and superconductivity, may coexist [38–43].

On the other hand, the multi-orbital feature could also give rise to non-unitary pairings, which again includes both time-reversal breaking (TRB) and time-reversal invariant (TRI) pairings. Prior studies have demonstrated the existence of spin-singlet non-unitary pairing states that break the inversion symmetry in Dirac materials [9]. One aim of this work is the generalization to unitary and non-unitary gap functions in a spin-singlet SC while preserving inversion symmetry, which

is possible exactly due to the multi-orbital degrees of freedom. In a SC with multiple orbitals, we find that the non-unitary pairing state is a mixed superconducting states with both orbital-independent pairings and orbital-dependent pairings. Recently, the interplay between orbital-independent pairings and spin-orbit coupling (SOC) have been shown to demonstrate the intriguing phenomenon of large in-plane upper critical field compared with the Pauli paramagnetic field for a two-dimensional SC. For example, the Type I Ising superconductivity in monolayer MoS_2 [44, 45] and NbSe_2 [46] and the Type II Ising superconductivity in monolayer stanene [47]. The interplay of spin-orbit coupling (SOC) and multi-orbital pairing gives rise to a plethora of interesting physics. However, to the best of our knowledge, the influence of the atomic SOC on the orbital-dependent pairings remain unsolved. Moreover, it is still unclear that if there exists a new type of spin-orbit-coupled superconductivity other than the family of Ising SCs.

Another main topic of this work is concerned with the TRB and magnetism in these SCs, emphasizing on the multi-orbital nature. It is well-known that spin-polarization (SP) can coexist with nonunitary *spin-triplet* superconductivity, which is believed to be the case for LaNiC_2 [48] and LaNiGa_2 [49, 50]. More recently, the coexistence of magnetism and *spin-singlet* superconductivity is experimentally suggested in multi-orbital SCs, such as iron-based superconductors [51, 52] and LaPt_3P [53]. Therefore, it will be interesting to examine how SP develops in multi-orbital spin-singlet SCs as spontaneous TRS breaking in the absence of external magnetic fields or Zeeman fields.

In this work, we address the above two major issues by studying a two-band SC with two atomic orbitals. A Ginzburg-Landau (GL) theory is constructed to exhibit

* hu.lunhui.zju@gmail.com

all the possible spin-singlet non-unitary pairing states. First and foremost, the influence of atomic spin-orbit coupling is studied, which gives birth to a new spin-orbit-coupled SC. This exotic state shows the following features: firstly, a large Pauli-limit violation is found for the orbital-independent pairing part, which belongs to the Type II Ising superconductivity. Furthermore, the orbital-dependent pairing part also shows a weak Pauli-limit violation even though it does not belong to the family of Ising SCs. Secondly, topological superconductivity can be realized with a physical set of parameters even in the absence of external magnetic fields or Zeeman fields. In addition, a spin-polarized superconducting state could be energetically favored with a spontaneous breaking of time-reversal symmetry. Our work implies a new mechanism to the establishment of spin magnetism in the spin-singlet SC. In the end, we also discuss how to detect this effect by spin-resolved scanning tunneling microscopy measurements.

The paper is organized as the following: in section II, we apply the GL mean-field theory to investigate the spin-singlet non-unitary pairing states. In section III, the effects of atomic SOC on such pairing states are extensively studied, as well as the in-plane paramagnetic depairing effect. Besides, the topological superconductivity are studied in section IV even in the absence of external magnetic fields or Zeeman fields, after which we consider the spontaneous TRB effects in section V and show that spin-singlet SC-induced spin magnetism could emerge in the presence of orbital SOC. In the end, a brief discussion and conclusion is given in section VI.

II. SPIN-SINGLET NON-UNITARY SUPERCONDUCTORS

In this section, we study a specific normal Hamiltonian with respect to both TRS and inversion symmetry, to investigate the orbital-dependent spin-singlet superconducting states when the system includes two atomic orbitals at the Fermi energy. In Ref. [10], it has been shown that the orbital-dependent pairings could be stabilized in crystals against orbital hybridization and repulsive interactions. In this work, we discuss how such pairings could give birth to the establishment of spin-singlet non-unitary pairings via a general Ginzburg-Landau theory. Practically, such pairings are further classified into two categories according to TRS.

Before proceeding, we briefly review both unitary and non-unitary gap functions for a single-band SC in the absence of inversion symmetry. In this case, a general singlet-triplet mixed pairing potential is given by

$$\hat{\Delta}(\mathbf{k}) = [\Delta_s \psi_s(\mathbf{k}) \sigma_0 + \Delta_t (\mathbf{d}_s(\mathbf{k}) \cdot \boldsymbol{\sigma})] (i\sigma_2), \quad (1)$$

where $\boldsymbol{\sigma}$ are Pauli matrices acting in the spin subspace. Here $\psi_s(\mathbf{k})$ represents even-parity spin-singlet pairings and the odd-parity $\mathbf{d}_s(\mathbf{k})$ is for the spin-triplet d_s -vector. Physically, the unitary SC has only one superconducting

gap like in the conventional BCS theory, while a two-gap feature comes into being by the non-unitary pairing potential. More explicitly, the unitary or non-unitary is defined by whether the following is proportional to the identity matrix σ_0 :

$$\begin{aligned} \hat{\Delta}(\mathbf{k}) \hat{\Delta}^\dagger(\mathbf{k}) &= |\Delta_s|^2 \psi_s^2 + |\Delta_t|^2 |\mathbf{d}_s|^2 \\ &+ 2\text{Re}[\Delta_s \Delta_t^* \psi_s \mathbf{d}_s^*] \cdot \boldsymbol{\sigma} + i|\Delta_t|^2 (\mathbf{d}_s \times \mathbf{d}_s^*) \cdot \boldsymbol{\sigma}, \end{aligned} \quad (2)$$

Therefore, Eq. (2) gives rise to a general classification by assuming a non-vanishing $\Delta_s \in \mathbb{R}$ and a proper choosing of a global gauge phase. In principle, there are four possible phases, including the time-reversal-invariant (TRI) non-unitary SCs ($\Delta_t \in \mathbb{R}, \mathbf{d}_s \in \mathbb{R}$), the time-reversal-breaking (TRB) unitary SCs ($\Delta_t \sim i, \mathbf{d}_s \in \mathbb{R}$); the TRI unitary SCs ($\Delta_t \in \mathbb{C}, \mathbf{d}_s \in \mathbb{R}$), and the TRB non-unitary SCs ($\Delta_t \in \mathbb{R}, \mathbf{d}_s \in \mathbb{C}$). These states might be distinguished in experiments, for example, the TRB unitary pairing state might induce a spontaneous magnetization with the help of Rashba spin-orbit coupling [54].

As we know, the spin-singlet pairings do not coexist with the spin-triplet pairings in the presence of inversion symmetry (e.g. centrosymmetric SCs). Roughly speaking, it seems out of the question to realize non-unitary pairing states in purely spin-singlet SCs. However, this is a challenge but not an impossibility for a SC with multi-orbitals, which is one of the aims of this work. In the following, we will discuss how to generalize the classification of TRI or TRB and unitary or non-unitary pairing states to a spin-singlet SC with two atomic orbitals in the presence of inversion symmetry.

A. Model Hamiltonians

Specifically, we consider a two-orbital system described by the inversion-symmetric Hamiltonian in two dimensions (2D),

$$\mathcal{H}_0(\mathbf{k}) = \epsilon(\mathbf{k}) + \lambda_{soc} \sigma_3 \tau_2 + \lambda_o \mathbf{g}_o \cdot \boldsymbol{\tau}, \quad (3)$$

where the basis is made of $\{d_{xz}, d_{yz}\}$ -orbitals $\psi_{\mathbf{k}}^\dagger = (c_{d_{xz}, \uparrow}^\dagger(\mathbf{k}), c_{d_{xz}, \downarrow}^\dagger(\mathbf{k}), c_{d_{yz}, \uparrow}^\dagger(\mathbf{k}), c_{d_{yz}, \downarrow}^\dagger(\mathbf{k}))$. Here $\boldsymbol{\tau}$ and $\boldsymbol{\sigma}$ are Pauli matrices acting on the orbital and spin subspace, respectively, and τ_0, σ_0 are 2-by-2 identity matrices. Besides, $\epsilon(\mathbf{k}) = -(k_x^2 + k_y^2)/2m - \mu$ is the band energy measured relative to the chemical potential μ , λ_{soc} is the atomic SOC [55] and λ_o characterizes the strength of orbital hybridization. In this work, the anisotropic effective mass has been ignored for simplicity, and the normalized $\mathbf{g}_o = (g_1, 0, g_3)$ is used to satisfy both TRS and inversion symmetry.

In addition, by ignoring the fluctuations, the mean-field pairing Hamiltonian is generally given by,

$$\mathcal{H}_\Delta = \sum_{\mathbf{k}, s_1 a, s_2 b} \Delta_{s_1, s_2}^{a, b}(\mathbf{k}) c_{s_1 a}^\dagger(\mathbf{k}) c_{s_2 b}^\dagger(-\mathbf{k}) + \text{h.c.}, \quad (4)$$

where s_1, s_2 are index for spin and a, b are for orbitals. Here c^\dagger is the creation operator of electrons. In analogy to spin-triplet SCs, we use an orbital $\mathbf{d}_o(\mathbf{k})$ -vector for the spin-singlet orbital-dependent pairing potential [12], which takes the generic form

$$\hat{\Delta}_{tot}(\mathbf{k}) = [\Delta_s \Psi_s(\mathbf{k}) \tau_0 + \Delta_o (\mathbf{d}_o(\mathbf{k}) \cdot \boldsymbol{\tau})] (i\sigma_2), \quad (5)$$

where Δ_s and Δ_o are pairing strengths in orbital-independent and orbital-dependent channels, respectively. The Fermi statistics requires that $\Psi_s(\mathbf{k}) = \Psi_s(-\mathbf{k})$, while the three components of \mathbf{d}_o satisfy $d_o^{1,3}(\mathbf{k}) = d_o^{1,3}(-\mathbf{k})$ and $d_o^2(\mathbf{k}) = -d_o^2(-\mathbf{k})$. Namely, $d_o^2(\mathbf{k})$ represents odd-parity spin-singlet orbital-singlet pairings and the others are for even-parity spin-singlet orbital-triplet pairings. Combining Eq. (5) with Eq. (3), the Bogoliubov-de-Gennes (BdG) Hamiltonian is

$$\mathcal{H}_{\text{BdG}} = \begin{pmatrix} \mathcal{H}_0(\mathbf{k}) & \hat{\Delta}_{tot}(\mathbf{k}) \\ \hat{\Delta}_{tot}^\dagger(\mathbf{k}) & -\mathcal{H}_0^*(-\mathbf{k}) \end{pmatrix}, \quad (6)$$

which is based on the Nambu basis $(\psi_{\mathbf{k}}^\dagger, \psi_{-\mathbf{k}}^T)$. Same with the spin case in Eq. (2), the non-unitarity of a spin-singlet pairing potential defined in Eq. (5) is determined by whether $\hat{\Delta}_{tot}(\mathbf{k})\hat{\Delta}_{tot}^\dagger(\mathbf{k})$ is proportional to an identity matrix. More explicitly we have

$$\begin{aligned} \hat{\Delta}_{tot}(\mathbf{k})\hat{\Delta}_{tot}^\dagger(\mathbf{k}) &= |\Delta_s|^2 \psi_s^2 + |\Delta_o|^2 |\mathbf{d}_o|^2 \\ &+ 2\text{Re}|\Delta_s \Delta_o^* \psi_s \mathbf{d}_o^*| \cdot \boldsymbol{\tau} + i|\Delta_o|^2 (\mathbf{d}_o \times \mathbf{d}_o^*) \cdot \boldsymbol{\tau}, \end{aligned} \quad (7)$$

which could also exhibit four general possibilities: TRI or TRB and unitary or non-unitary SCs, with a simple replacement $\{\Delta_t, \mathbf{d}_s\} \rightarrow \{\Delta_o, \mathbf{d}_o\}$. In the absence of band splittings, i.e., $\lambda_{soc} = \lambda_0 = 0$ as an illustration, the superconducting excitation gaps on the Fermi surfaces of a TRI unitary SC are

$$E_{\alpha, \beta}(\mathbf{k}) = \alpha \sqrt{\epsilon^2(\mathbf{k}) + (\Delta_s \psi_s(\mathbf{k}) + \beta \Delta_o |\mathbf{d}_o|)^2}, \quad (8)$$

with $\alpha, \beta = \pm$. It is similar to the superconducting gaps for non-unitary spin-triplet SCs [1]. Moreover, the two-gap feature indicates the non-unitarity of the superconducting states, which implies the possibility of a nodal SC as long as $\Delta_s \psi_s(\mathbf{k}) \pm \Delta_o |\mathbf{d}_o| = 0$ is satisfied on the Fermi surfaces. And, the nodal quasi-particle states can be experimentally detected by measuring specific heat, London penetration depths, μSR , NMR, etc. As a result, this provides a possible evidence to get a sight of TRI non-unitary phases in real materials (e.g. centrosymmetric SCs). Furthermore, the above conclusion is still valid when we turn on λ_{soc} and λ_0 .

B. Superconducting phase diagrams

In this subsection, we explore a possible superconducting phase diagram including the non-unitary pairing states. Here we assume a two-band SC with

$$\hat{\Delta}_{tot} = [\Delta_s \tau_0 + \Delta_o (d_o^1 \tau_1 + d_o^3 \tau_3)] (i\sigma_2). \quad (9)$$

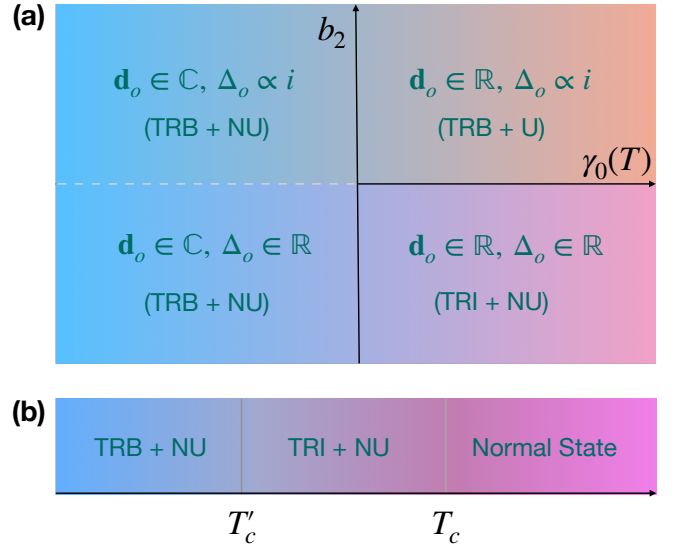


FIG. 1. Schematic superconducting phase diagrams. (a) shows the phase diagram on the b_2 - $\gamma_0(T)$ plane when $b_1 = 0$ and Δ_s is real and non-zero. And (b) exhibits a possible phase diagram as a function of temperature, indicating the transition from a TRI NU state to a TRB NU state. It corresponds to the $b_2 < 0$ case in (a). Here, TRB and TRI are short for TR-breaking and TR-invariant, respectively; U and NU represent unitary and non-unitary, respectively.

In terms of the superconducting order parameters $\{\Delta_s, \Delta_o, \mathbf{d}_o = (d_o^1, 0, d_o^3)\}$ and the order parameter for the orbital orderings $\mathbf{M}_o \propto \sum_{\mathbf{k}, \sigma} (c_{\sigma a}^\dagger(\mathbf{k}) \boldsymbol{\tau}_{ab} c_{\sigma b}(\mathbf{k}))$, the total GL free energy can be constructed to address the homogeneous superconducting phase without external magnetic fields [10]

$$\mathcal{F}[\Delta_s, \Delta_o, \mathbf{d}_o, \mathbf{M}_o] = \mathcal{F}_0 + \mathcal{F}_b + \mathcal{F}_o, \quad (10)$$

where

$$\begin{aligned} \mathcal{F}_0 &= \frac{1}{2} \alpha(T) (|\Delta_o|^2 + |\Delta_s|^2) + \frac{1}{2} \alpha_M |\mathbf{M}_o|^2 \\ &+ \frac{1}{4} \beta |\Delta_o|^4 + \frac{1}{4} \beta' |\Delta_s|^4 + \beta'' |\Delta_s|^2 |\Delta_o|^2 \\ &+ \beta_o |d_o^1|^4 + \beta'_o |d_o^3|^4, \end{aligned} \quad (11)$$

where $|\mathbf{d}_o| = 1$ is adopted, $\alpha(T) = \alpha_0(T/T_c - 1)$ and the coefficients $\alpha_0, \alpha_M, \beta, \beta', \beta'', \beta_o, \beta'_o$ are all positive. For simplicity, the same critical temperature T_c is assumed in both orbital-independent and orbital-dependent channels. And $\alpha_M > 0$ means that there is no spontaneous atomic orbital polarization. In the superconducting state with both non-zero Δ_s and Δ_o developed already, additionally, there are two possible ways to pursue the spontaneous TRB, denoted as \mathcal{F}_b and \mathcal{F}_o . Firstly, we consider the \mathcal{F}_b term

$$\mathcal{F}_b = b_1 \Delta_s^* \Delta_o + b_2 (\Delta_s^* \Delta_o)^2 + \text{h.c.}, \quad (12)$$

where the sign of b_2 determines the breaking of TRS. Given by $b_1 = 0$ and $b_2 > 0$, we have a $\theta_o = \pm\pi/2$

relative phase difference between Δ_s and $\Delta_o e^{i\theta_o}$ [56], which gives to the achievement of the TRB unitary pairing state ($\Delta_s \in \mathbb{R}, \Delta_o \sim i, \mathbf{d}_o \in \mathbb{R}$). More generally, a TRB non-unitary SC arises from the non-zero bilinear b_1 -term, which is symmetry-allowed only when Δ_s and Δ_o belong to the same symmetry representation of the crystalline symmetry group. Namely, the case with $b_1 \neq 0$ and $b_2 > 0$ can pin the phase difference θ_o to an arbitrary nonzero value, i.e., $\theta_o \in (0, \pi)$. On the other hand, the $b_2 < 0$ situation makes TRI non-unitary pairing states ($\Delta_s \in \mathbb{R}, \Delta_o \in \mathbb{R}, \mathbf{d}_o \in \mathbb{R}$).

However, even in the case with $b_2 < 0$, we still have an alternative approach to reach TRB pairing states, driven by the \mathcal{F}_o term

$$\mathcal{F}_o = \gamma_0(T) |\mathbf{d}_o \times \mathbf{d}_o^*|^2 + i\gamma_1 \mathbf{M}_o \cdot (\mathbf{d}_o \times \mathbf{d}_o^*) + \text{h.c.}, \quad (13)$$

where the sign of $\gamma_0(T)$ identifies the TRB. If we set $\gamma_0(T) = \gamma_0(T/T'_c - 1)$ with $\gamma_0 > 0$ and $T'_c < T_c$, i.e., T'_c is the critical temperature for the spontaneous TRB inside the superconducting states. Thus, $\gamma_0(T) < 0$ results in a TRB non-unitary state ($\Delta_s \in \mathbb{R}, \Delta_o \in \mathbb{R}, \mathbf{d}_o \in \mathbb{C}$).

As a brief conclusion, all the above discussed pairing states are summarized in Fig. 1(a), which schematically shows a superconducting phase diagram as a function of b_2 and $\gamma_0(T)$ by simply setting $b_1 = 0$. Moreover, the possible phase diagram as a function of temperature in Fig. 1(b) exhibits the transition from a TRI non-unitary SC to a TRB non-unitary SC.

III. THE PAULI LIMIT VIOLATION: A LARGE IN-PLANE UPPER CRITICAL FIELD

In this section, we study the Pauli limit violation for the spin-singlet TRI non-unitary SC against an in-plane magnetic field (e.g. $H_{c2,\parallel} > H_P$). For a 2D crystalline SC or a thin film SC, the realization of superconducting states that are resilient to a strong external magnetic field has remained a significant pursuit, namely, the pairing mechanism can remarkably enlarge the in-plane upper critical field. Along this crucial research direction, one recent breakthrough has been the identification of ‘‘Ising pairing’’ formed with the help of Ising-type spin-orbit coupling (SOC), which breaks the SU(2) spin rotation and pins the electron spins to the out-of-plane direction. Depending on whether the inversion symmetry is broken or not by the Ising-type SOC, the Ising pairing is classified as Type I (broken) and Type II (preserved) Ising superconductivity, where the breaking of Cooper pairs is difficult under an in-plane magnetic field.

For this purpose, in the following, we consider the interplay between atomic SOC $\lambda_{soc} \neq 0$ and spin-singlet TRI non-unitary pairing state in Eq. (9). Another reason for studying the atomic SOC is that it is not negligible in many real materials. Without loss of generality, the direction of the magnetic field can be taken to be the x -direction, i.e., $\mathbf{H} = (H_x, 0, 0)$ with $H_x \geq 0$. Therefore,

the normal Hamiltonian becomes

$$\mathcal{H}_0(\mathbf{k}) = \epsilon(\mathbf{k}) + \lambda_{soc} \sigma_3 \tau_2 + \lambda_o \mathbf{g}_o \cdot \boldsymbol{\tau} + h \sigma_1 \tau_0, \quad (14)$$

where $h = \frac{1}{2} g \mu_B H_x$ is the Zeeman energy with $g = 2$ the electron’s g -factor. To explicitly investigate the violation of Pauli limit for the spin-orbit coupled SCs, we calculate the in-plane upper critical magnetic field normalized to the Pauli-limit paramagnetic field $H_{c2,\parallel}/H_P$ as a function of the normalized temperature T_c/T_0 , by solving the linearized gap equation. Here $H_P = 1.86T_0$ represents the Pauli limit with T_0 the critical temperature in the absence of external magnetic field.

Following the standard BCS decoupling scheme [10], we first solve T_c for the orbital-independent pairing channel by solving the linearized gap equation, $v_0 \chi_s(T) - 1 = 0$, where v_0 is effective attractive interaction and the superconductivity susceptibility $\chi_s(T)$ is defined by

$$\chi_s(T) = -\frac{1}{\beta} \sum_{\mathbf{k}, \omega_n} \text{Tr} \left[G_e(\mathbf{k}, i\omega_n) G_h(-\mathbf{k}, i\omega_n) \right], \quad (15)$$

where the conventional s-wave pairing with $\psi_s(\mathbf{k}) = 1$ is considered. Here $G_e(\mathbf{k}, i\omega_n) = [i\omega_n - \mathcal{H}_0(\mathbf{k})]^{-1}$ is the Matsubara Green’s function for electrons and that for holes is defined as $G_h(\mathbf{k}, i\omega_n) = -\sigma_2 G_e^*(\mathbf{k}, i\omega_n) \sigma_2$. Here $\beta = 1/k_B T$ and $\omega_n = (2n+1)\pi/\beta$ with n integer. Likewise, for the orbital-dependent pairing channels, the superconductivity susceptibility $\chi_o(T)$ is defined as

$$\chi_o(T) = -\frac{1}{\beta} \sum_{\mathbf{k}, \omega_n} \text{Tr} \left[(\mathbf{d}_o(\mathbf{k}) \cdot \boldsymbol{\tau})^\dagger G_e(\mathbf{k}, i\omega_n) \right. \\ \left. \times (\mathbf{d}_o(\mathbf{k}) \cdot \boldsymbol{\tau}) G_h(-\mathbf{k}, i\omega_n) \right]. \quad (16)$$

The coupling between orbital-independent and orbital-dependent channels leads to a high-order correction ($\sim \lambda_o^2/\mu^2$), which can be ignored once $\lambda_o \ll \mu$.

A. Type II Ising superconductivity

In this subsection, we first consider the orbital-independent pairing state that becomes a Type II Ising SC with the help of the atomic SOC λ_{soc} . After a straightforward calculation (Appendix A), the superconductivity susceptibility $\chi_s(T)$ in Eq. (15) is calculated as

$$\chi_s(T) = \chi_0(T) + N_0 f_s(T, \lambda_{soc}, \lambda_o, h), \quad (17)$$

with N_0 is the DOS near the Fermi surface and the pair-breaking term is given by

$$f_s(T, \lambda_{soc}, \lambda_o, h) = \frac{1}{2} [\mathcal{C}_0(T, \rho_-) + \mathcal{C}_0(T, \rho_+)] \\ + [\mathcal{C}_0(T, \rho_-) - \mathcal{C}_0(T, \rho_+)] \left(\frac{\lambda_{soc}^2 + \lambda_o^2 - h^2}{2E_+ E_-} \right), \quad (18)$$

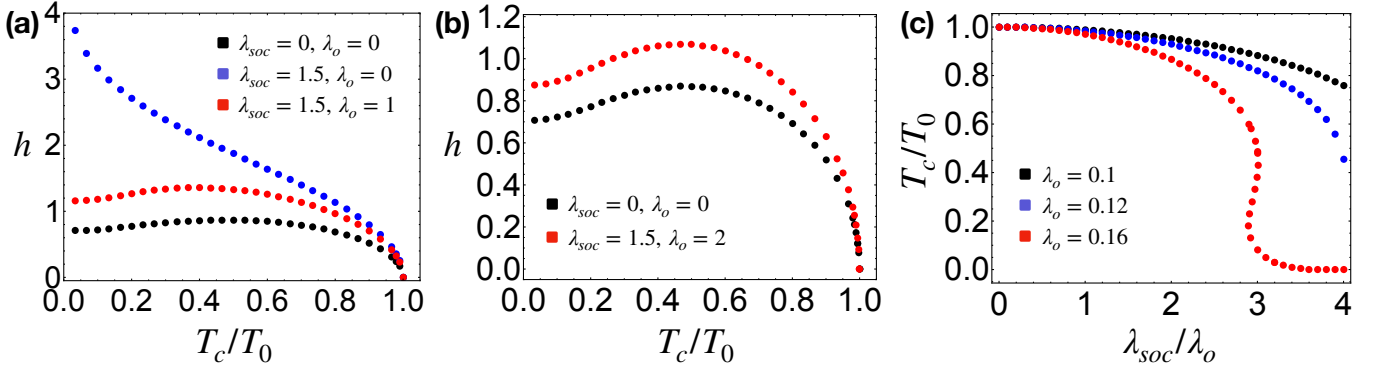


FIG. 2. The pair-breaking effects. (a) A significant Pauli limit violation due to the atomic SOC for the orbital-independent pairing. Parameters used: $\Delta_s = 1$, $\mathbf{g}_o = (1, 0, 1)$. (b) A weak Pauli limit violation due to the atomic SOC for the orbital-dependent pairing. Parameters used: $\Delta_o = 1$, $\mathbf{d}_o = (1, 0, 1)$, $\mathbf{g}_o = (1, 0, 1)$. (c) The suppression of T_c by atomic SOC for orbital-dependent pairing at zero external magnetic field. Parameters used: $\Delta_o = 1$, $\mathbf{d}_o = (1, 0, 1)$, $\mathbf{g}_o = (1, 0, 1)$.

where $E_{\pm} \equiv \sqrt{\lambda_{soc}^2 + (\lambda_o \pm h)^2}$, $\rho_{\pm} = \frac{1}{2}(E_+ \pm E_-)$, and $\chi_0(T) = N_0 \ln\left(\frac{2e^{\gamma}\omega_D}{\pi k_B T}\right)$ is the superconducting susceptibility when $\lambda_{soc}, \lambda_o, h = 0$. Here $\gamma = 0.57721 \dots$ is the Euler-Mascheroni constant. Furthermore, the kernel function of the pair-breaking term f_s is given by

$$C_0(T, E) = \text{Re} \left[\psi^{(0)}\left(\frac{1}{2}\right) - \psi^{(0)}\left(\frac{1}{2} + i\frac{E}{2\pi k_B T}\right) \right], \quad (19)$$

with $\psi^{(0)}(z)$ being the digamma function. Note that $C_0(T, E) \leq 0$ and it monotonically decreases as E increases, indicating the reduction of T_c . Namely, $C_0(T, E)$ gets smaller for a larger E .

We first discuss the simplest case with $\lambda_{soc} = \lambda_o = 0$, where the pair-breaking function becomes $f_s(T, 0, 0, h) = C_0(T, h)$, which just leads to the Pauli limit $H_{c2, \parallel} \approx H_P = 1.86T_c$, as shown in Fig. 2(a). Furthermore, we turn on λ_{soc} while take the $\lambda_o \rightarrow 0$ limit, the pair-breaking term in Eq. (18) is reduced to

$$f_s(T, \lambda_{soc}, 0, h) = C_0\left(T, \sqrt{\lambda_{soc}^2 + h^2}\right) \frac{h^2}{\lambda_{soc}^2 + h^2}, \quad (20)$$

which reproduces the same results of Type II Ising superconductors in Ref. [57]. Under a relatively weak magnetic field ($h \ll \lambda_{soc}$), the factor $h^2/(\lambda_{soc}^2 + h^2) \ll 1$ leads to $f_s(T, \lambda_{soc}, 0, h) \rightarrow 0$, which in turn induces a large in-plane $H_{c2, \parallel}/H_P$.

Next, we investigate the effect of the spin-independent orbital hybridization λ_o on the in-plane upper critical field $H_{c2, \parallel}$. Interestingly, λ_o would instead reduce $H_{c2, \parallel}$. To see it explicitly, we expand the pair-breaking function f_s in Eq. (18) up to the leading order of λ_o^2 ,

$$f_s(T, \lambda_{soc}, \lambda_o, h) \approx f_s(T, \lambda_{soc}, 0, h) + F(T, \lambda_{soc}, h)\lambda_o^2, \quad (21)$$

where $F(T, \lambda_{soc}, h)$ is given in the Appendix A and we find it is always negative ($F(T, \lambda_{soc}, h) < 0$). In addition to the first term $f_s(T, \lambda_{soc}, 0, h)$ discussed in Eq. (20),

the second term $\Delta_{\lambda} h^2 \lambda_o^2$ also serves as a pair-breaking effect on T_c at non-zero field. Therefore, the second λ_o -term further reduces T_c , leading to the reduction of the in-plane upper critical field.

We then numerically confirm the above discussions. We solve the linearized gap equation $v_0 \chi_s(T) - 1 = 0$ and arrive at $\log(T_c/T_0) = f_s(T_c, \lambda_{soc}, \lambda_o, h)$, from which T_c/T_0 is numerically calculated in Fig. 2(a). Here T_0 is the critical temperature at zero external magnetic field. The Pauli limit corresponds to $T_0(\lambda_{soc} = 0, \lambda_o = 0, h = 0)$. We see that in general there is Pauli limit violation for non-zero λ_{soc} and λ_o . Furthermore, by comparing the two cases with $\lambda_{soc} = 1.5, \lambda_o = 0$ and $\lambda_{soc} = 1.5, \lambda_o = 1$, we confirm the above approximated analysis.

B. A weakly enhanced in-plane $H_{c2, \parallel}$ compared to Pauli limit

In this subsection, we demonstrate the influence of the atomic SOC λ_{soc} on the paramagnetic pair-breaking effect for orbital-dependent pairings. We find a weak enhancement of in-plane upper critical field compared with the Pauli limit. Following the criteria of the orbital \mathbf{d}_o -vector in Ref. [10], we take \mathbf{d}_o to be parallel to the orbital hybridization vector \mathbf{g}_o by assuming $\lambda_{soc} \ll \lambda_o$. This would be justified in the next subsection. After a straightforward calculation (Appendix A), the superconductivity susceptibility $\chi_o(T)$ in Eq. (16) is calculated as,

$$\chi_o(T) = \chi_0(T) + N_0 f_o(T, \lambda_{soc}, \lambda_o, h), \quad (22)$$

where the pair-breaking term is given by

$$f_o(T, \lambda_{soc}, \lambda_o, h) = \frac{1}{2} [C_0(T, \rho_-) + C_0(T, \rho_+)] + [C_0(T, \rho_-) - C_0(T, \rho_+)] \left(\frac{\lambda_o^2 - \lambda_{soc}^2 - h^2}{2E_+ E_-} \right), \quad (23)$$

which differs from $f_s(T, \lambda_{soc}, \lambda_o, h)$ for orbital-independent pairings in Eq. (18). The only difference between them lies in the factor $(\lambda_o^2 - \lambda_{soc}^2 - h^2)/2E_+E_-$, compared with that of $f_s(T, \lambda_{soc}, \lambda_o, h)$ (i.e. $(\lambda_o^2 + \lambda_{soc}^2 - h^2)/2E_+E_-$), which leads to a completely distinct superconducting state, demonstrated as follows.

To understand Eq. (23), we first discuss the simplest case with $\lambda_{soc} = \lambda_o = 0$, where the pair-breaking function becomes $f(T, 0, 0, h) = C_0(T, h)$, which just leads to the Pauli limit $H_{c2, \parallel} \approx H_P = 1.86T_c$, as shown in Fig. 2(b). Likewise, this conclusion remains valid for $\lambda_{soc} = 0$ and $\lambda_o \neq 0$. Therefore, the Pauli-limit of in-plane upper critical field is not affected by λ_o itself.

On the other hand, if we turn on merely the atomic SOC $\lambda_{soc} \neq 0$ while keeping $\lambda_o = 0$, the pair-breaking function is given by

$$f_o(T, \lambda_{soc}, 0, h) = C_0(T, \sqrt{\lambda_{soc}^2 + h^2}), \quad (24)$$

which leads to the reduction of upper critical field, i.e., $H_{c2, \parallel} < H_P$, because of $f(T, \lambda_{soc}, 0, h) < f(T, 0, 0, h) < 0$. Because the atomic SOC also plays a similar role of “magnetic field” to suppress the orbital-dependent pairing, as discussed in the next subsection. Thus, it does not belong to the family of Ising SCs, which makes the orbital-dependent pairing significantly different from the orbital-independent pairings.

However, it is surprising to notice that there is actually a weak enhancement of the in-plane upper critical field $H_{c2, \parallel}$ for the case with both $\lambda_o \neq 0$ and $\lambda_{soc} \neq 0$. Solving the gap equation $v_0\chi_o(T) - 1 = 0$, we obtain

$$\ln\left(\frac{T_c}{T_0}\right) = f_o(T, \lambda_{soc}, \lambda_o, h). \quad (25)$$

Fig. 2(b) shows how T_c/T_0 changes with applied in-plane magnetic field, where the Pauli limit curve corresponds to $\lambda_{soc}, \lambda_o = 0$. When both the atomic SOC and orbital hybridization are included, the critical field H_{c2} exceeds the Pauli limit by a small margin. Therefore, a spin-orbit-coupled SC with spin-singlet non-unitary pairing symmetries does not belong to the reported family of Ising superconductivity.

C. Atomic SOC induced zero-field Pauli limit

As mentioned above, the atomic SOC breaks the spin degeneracy, which generally suppresses the even parity orbital-dependent pairings. Thus, the robustness of spin-singlet non-unitary pairings in the presence of atomic SOC is the preliminary issue that we need to address. And we find that the spin-singlet TRI non-unitary pairing is also prevalent in solid state systems when the energy scale of atomic SOC is smaller than that of the orbital hybridization. In this case, we focus on the zero magnetic field limit. Using the general results from the

calculations in the previous section, we have

$$\begin{aligned} \ln\left(\frac{T_c}{T_0}\right) &= f_o(T, \lambda_{soc}, \lambda_o, h = 0) \\ &= C_0\left(T, \sqrt{\lambda_o^2 + \lambda_{soc}^2}\right) \frac{\lambda_{soc}^2}{\lambda_o^2 + \lambda_{soc}^2}, \end{aligned} \quad (26)$$

where $C_0(T, E)$ is defined in Eq. (19). In the case of $\lambda_{soc} = 0$, it can be seen that $T_c(\lambda_o) = T_0(\lambda_o = 0)$, i.e. the superconducting T_c is not suppressed by the orbital hybridization λ_o when the orbital \mathbf{d}_o -vector is parallel to the orbital hybridization vector \mathbf{g}_o [10]. However, in the presence of non-zero atomic SOC λ_{soc} , the T_c will be suppressed even when $\mathbf{d}_o \parallel \mathbf{g}_o$ is satisfied. Fig. 2(c) shows the behavior of T_c as a function of the λ_{soc}/λ_o for two different values of λ_o . We see the suppression of T_c as long as $\lambda_{soc} \neq 0$, and the suppression is more prominent when λ_o is larger.

To understand the suppression of orbital-dependent pairings by the atomic SOC, we take the $\lambda_o = 0$ limit. Eq. (26) leads to

$$\ln\left(\frac{T_c}{T_0}\right) = C_0(T, \lambda_{soc}), \quad (27)$$

which implies that λ_{soc} plays the same role of “magnetic field” that suppresses the T_c of the orbital-dependent pairing states. And $\lambda_{soc} \sim H_P$ roughly measure the zero-field “Pauli-limit” of the orbital-dependent pairing states. Motivated by this observation, we notice that the normal Hamiltonian given in Eq. (3) satisfies $[\mathcal{H}_0, \tau_2] = 0$ with $\lambda_o \rightarrow 0$. As a result, we can project the normal Hamiltonian \mathcal{H}_0 in Eq. (3) into block-diagonal form corresponding to the ± 1 eigenvalues of τ_2 by using the basis transformation

$$\mathcal{U} = \sigma_0 \otimes \frac{1}{\sqrt{2}} \begin{bmatrix} 1 & -i \\ 1 & i \end{bmatrix}. \quad (28)$$

The new basis is given by

$$\tilde{\Psi}^\dagger(\mathbf{k}) = (c_{+, \uparrow}^\dagger, c_{+, \downarrow}^\dagger, c_{-, \downarrow}^\dagger, c_{-, \uparrow}^\dagger), \quad (29)$$

where $c_{\pm, s}^\dagger \equiv \frac{1}{\sqrt{2}}(c_{dxz, s}^\dagger \mp ic_{dyz, s}^\dagger)$. In this basis, the normal Hamiltonian is given by

$$\mathcal{H}_0 = \mathcal{H}_0^+ \oplus \mathcal{H}_0^-, \quad (30)$$

where \mathcal{H}_0^\pm are given by

$$\mathcal{H}_0^\pm = \epsilon(\mathbf{k}) \mp \lambda_{soc} \sigma_3. \quad (31)$$

Note that the time-reversal transforms $\mathcal{H}_0^\pm(\mathbf{k})$ to $\mathcal{H}_0^\mp(-\mathbf{k})$. Explicitly, the atomic SOC is indeed magnetic field in each subspace, while it switches sign in the two subspaces to conserve TRS. In the new basis the pairing Hamiltonian also decouples as $\mathcal{H}_\Delta = \mathcal{H}_\Delta^+ \oplus \mathcal{H}_\Delta^-$ with \mathcal{H}_Δ^\pm given by

$$\mathcal{H}_\Delta^\pm = 2\Delta_\pm \left[c_{\pm, \uparrow}^\dagger(\mathbf{k})c_{\pm, \downarrow}^\dagger(-\mathbf{k}) - (\uparrow \leftrightarrow \downarrow) \right] + \text{h.c.}, \quad (32)$$

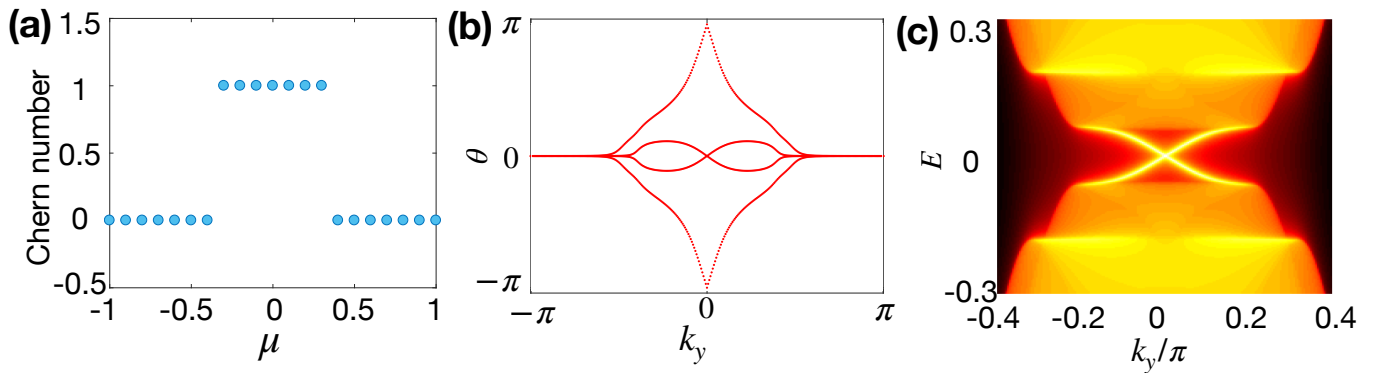


FIG. 3. Topological helical superconductivity for spin-singlet orbital-dependent pairing in the presence of Rashba SOC. (a) Z_2 index calculated by decoupling the BdG Hamiltonian into two chiral blocks when $\Delta_s = 0$ and $\lambda_o = 0$. The other parameters used: $t_0 = 1$, $\mu = 0.2$, $\lambda_{soc} = 0.4$, $\lambda_R = 1$, $\Delta_o = 0.1$, $\mathbf{d}_o = (1, 0, 1)$, $\mathbf{g}_o = (1, 0, 1)$. (b) Wilson loop calculation of the Z_2 invariant for $\Delta_s = 0.05$ and $\lambda_o = 0.1$. The other parameters remain the same as in (a). (c) Two counter-propagating Majorana edge states of the helical TSC.

where $\Delta_{\pm} \equiv \Delta_o(\mp id_o^1 + d_o^3)$ are the gap strengths in each subspace. In each subspace, it resembles an s-wave superconductor under a magnetic field along the out-of-plane direction. It explains the “Pauli-limit” pair-breaking effect of atomic SOC on the orbital-dependent pairings with the $\lambda_o \rightarrow 0$ limit. As a brief conclusion, our results demonstrate that the spin-singlet non-unitary SC with orbital-dependent pairings occurs only in a weak atomic SOC electronic systems.

IV. HELICAL SUPERCONDUCTIVITY

In the above sections, the spin-orbit-coupled SCs with respect to inversion symmetry have been studied. Then, it will be natural to ask if there exist more interesting superconducting states (e.g. topological phases) by including an inversion-symmetry breaking to the normal Hamiltonian. For this purpose, in this section, we focus on the Rashba SOC and explore its effect on the spin-orbit-coupled SCs. Even though the 2D bulk SC or thin film SC preserves the inversion symmetry, a Rashba SOC appears near an interface between the superconducting layer and the insulating substrate. Remarkably, we find a TRI topological SC (helical TSC) phase generated by the interplay between the two types of SOC (atomic and Rashba) and spin-singlet orbital-dependent pairings. Since TRS is preserved, it belongs to Class DIII according to the ten-fold classification. On the boundary of the interface, there exist a pair of helical Majorana edge states [58–67].

We now consider a Rashba SOC at the interface, which is described by

$$\mathcal{H}_0(\mathbf{k}) = \epsilon(\mathbf{k}) + \lambda_{soc}\sigma_3\tau_2 + \lambda_o\mathbf{g}_o \cdot \boldsymbol{\tau} + \lambda_R\mathbf{g}_R \cdot \boldsymbol{\sigma}, \quad (33)$$

where λ_R is the strength of the Rashba SOC with $\mathbf{g}_R = (-k_y, k_x)$. And we consider the TRI spin-singlet non-unitary pairing symmetry in Eq. (9) for the BdG Hamil-

tonian (6), namely, a real orbital \mathbf{d}_o -vector is assumed for the orbital-dependent pairings.

In the $\lambda_o \rightarrow 0$ and $\Delta_s \rightarrow 0$ limit, the bulk band gap closes at the Γ -point for $\mu_c^{\pm} = \pm\sqrt{\lambda_{soc}^2 - 4|\Delta_o|^2}$ while no gap-closing happens at other TRI momenta, leading to a topological phase transition. Thus, we conclude that the topological conditions are $\mu_c^- < \mu < \mu_c^+$ and an arbitrary orbital \mathbf{d}_o -vector. In the Appendix B, we show the Z_2 topological invariant can be analytically mapped to a BdG-version spin Chern number, similar to the spin Chern number in the 2D topological insulators. As mentioned in Sec. III(c), the conservation of τ_2 leads to the decomposition of the BdG Hamiltonian into two blocks with respect to different eigenvalues of τ_2 . In each subspace, we define the BdG Chern number as

$$\mathcal{C}_{\pm} = \frac{1}{2\pi} \sum_{\text{filled bands}} \int_{BZ} d\mathbf{k} \cdot \langle \phi_n^{\pm}(\mathbf{k}) | i\nabla_{\mathbf{k}} | \phi_n^{\pm}(\mathbf{k}) \rangle, \quad (34)$$

with $|\phi_n^{\pm}\rangle$ being the energy eigenstate of \mathcal{H}_{BdG}^{\pm} . Then the Z_2 topological invariant in this case is then explicitly given by,

$$\nu \equiv \frac{\mathcal{C}_+ - \mathcal{C}_-}{2}, \quad (35)$$

where \mathcal{C}_{\pm} are the Chern numbers of the \pm channels. $\nu = 1$ corresponds to the TSC phase, shown in Fig. 3(a). Based on the analysis for the topological condition, we learn that Δ_o should be smaller than λ_{soc} . However, as shown in Sec. III, the atomic SOC actually will reduce the T_c of orbital-dependent pairings, which set a guideline to a physically realizable set of parameters, $T_0 \gg \lambda_{soc} \gg \Delta_o$, beyond the BCS theory ($\Delta_o \sim 1.76T_0$). For example, the monolayer FeSe superconductor films on different substrates achieve a very high critical temperature $T_0 \sim 70$ K [68].

As for a more general case with non-zero λ_o and Δ_s , the BdG Hamiltonian can no longer be decomposed into

two decoupled blocks, hence the Chern number approach fails to characterize the Z_2 invariant. However, the more general Wilson-loop approach still works (see Appendix C). In general, the Z_2 -type topological invariant of a helical superconductivity could be characterized by the Wilson loop spectrum [69, 70], shown in Fig. 3(b), which demonstrates the non-trivial Z_2 index. To verify the helical topological nature, we calculate the edge spectrum in a semi-infinite geometry with k_y being a good quantum number. Fig. 3(c) confirms clearly that there is a pair of 1D helical Majorana edge modes (MEMs) propagating on the boundary of the 2D system.

V. TRB NON-UNITARY SUPERCONDUCTOR

So far, the TRI non-unitary pairing states are investigated, which exhibit the Pauli-limit violation for in-plane upper critical field and topological phases. Furthermore, in this section, we study the TRB non-unitary pairing states characterized by a complex \mathbf{d}_o -vector when both Δ_s and Δ_o are real. Here is what we want to address, as it is well known, the experiments by zero-field muon-spin relaxation (μ SR) and the polar Kerr effect (PKE) can provide a strong evidence to the observation of spontaneous magnetization or spin polarization in the superconducting states, which indicates a TRB superconducting pairing symmetry. On the theory side, the non-unitary spin-triplet pairing potentials are always adopted to explain the experiments. However, for a spin-singlet SC, a theory with TRB pairing induced spin-magnetization is in a great demand. Addressing this crucial issue is one of the aims of this work, and we find that a spin-singlet TRB non-unitary SCs supports a TRB atomic orbital polarization, which in turn would give rise to spin polarization in the presence of atomic SOC.

A. TRB and chiral TSC

In this subsection, we first explore the possible chiral topological phases by considering the simplest case with $\lambda_o = \Delta_s = 0$ to demonstrate the essential physics. For the TRB non-unitary pairing, a complex orbital \mathbf{d}_o -vector can be generally parametrized as $\mathbf{d}_o = (\cos \theta, 0, e^{i\phi} \sin \theta)$. And the relative phase $\phi = \pm\pi/2$ is energetically favored by minimizing the free energy in Eq. (13).

At the Γ point, the bulk gap closes at $\mu_{c,i}^\pm = \pm\sqrt{\lambda_{soc}^2 - 4|\Delta_i|^2}$, where $i = 1, 2$ and $\Delta_{1,2} = i\Delta_o(\sin \theta \pm \cos \theta)$. Due to TRB, $\mu_{c,1}^\pm \neq \mu_{c,2}^\pm$. Accordingly, we semi-qualitatively map out the phase diagram in Fig. 4 by tuning θ and μ , and label the different phase regions by the number of Majorana edge modes (MEMs), denoted as \mathcal{Q} . When $|\mu| > \max\{|\mu_{c,1}|, |\mu_{c,2}|\}$, the topologically trivial phase is achieved with $\mathcal{Q} = 0$. As for $\min\{|\mu_{c,1}|, |\mu_{c,2}|\} < |\mu| < \max\{|\mu_{c,1}|, |\mu_{c,2}|\}$, there is only one MEM on the boundary, corresponding to the $\mathcal{Q} = 1$ regions [71, 72].

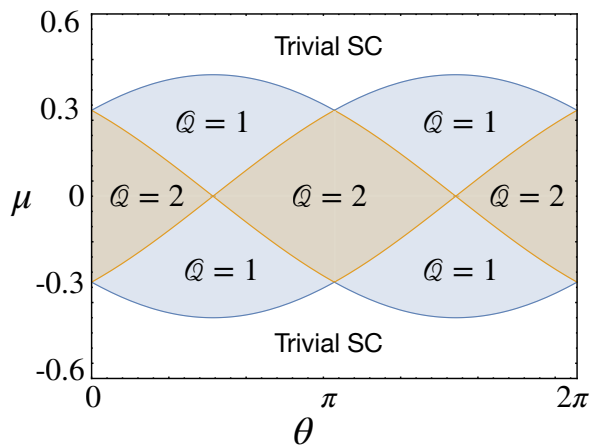


FIG. 4. Topological chiral superconductivity. We plot the phase diagram in terms of the number of MEMs (\mathcal{Q}) of the TSC. Parameters used: $\Delta_o = 0.14$, $\lambda_{soc} = 0.4$, $\phi = \pm\pi/2$, $\lambda_o = 0$ and $\Delta_s = 0$.

When $|\mu| < \min\{|\mu_{c,1}|, |\mu_{c,2}|\}$, there are $\mathcal{Q} = 2$ MEMs. The chiral TSC might be detected by anomalous thermal Hall conductivity $K_{xy} = \frac{\mathcal{Q}}{2} \frac{\pi T}{6}$ [73].

B. Atomic orbital polarization and spin polarization

Next, we show how spin-singlet TRB non-unitary pairing can induce spin polarization, and discuss how to identify such pairings by using spin-polarized scanning tunneling microscopy measurements. As discussed in the Ginzburg-Landau theory in Sec. II, for $T < T'_c$, a TRB complex orbital \mathbf{d}_o -vector generates the orbital orderings as

$$\mathbf{M}_o = -i\gamma_1/\alpha_M(\mathbf{d}_o \times \mathbf{d}_o^*), \quad (36)$$

of which the y -component breaks TRS shown in Fig. 5(a). More precisely, $M_o^y \propto \sum_{\mathbf{k}, \sigma} \langle \hat{n}_{\sigma, d_{xz} + id_{yz}}(\mathbf{k}) - \hat{n}_{\sigma, d_{xz} - id_{yz}}(\mathbf{k}) \rangle \neq 0$ indicates the atomic orbital-polarization (AOP). Here, \hat{n} is the density operator of electrons. Once M_o^y develops a finite value, it leads to orbital-polarized DOS and two distinct superconducting gaps of the quasi-particle spectrum (Fig. 5(c), more details below). Therefore, the orbital degree of freedom in spin-singlet SCs plays a similar role as the spin degree of freedom of spin-triplet SCs.

Once the atomic SOC is present, the spin-polarization (SP) could be induced indirectly,

$$\Delta\mathcal{F} = \alpha_s |\mathbf{M}_s|^2 + \gamma_{soc} M_s^z M_o^y, \quad (37)$$

with $\alpha_s > 0$ and $\gamma_{soc} \neq 0$. Here, $M_s^z \propto \sum_{\mathbf{k}, \tau} \langle \hat{n}_{\uparrow, \tau} - \hat{n}_{\downarrow, \tau} \rangle$. Therefore, the complex orbital \mathbf{d}_o -vector can be identified by spin-resolved density of states (DOS) for spin-singlet superconductors. In addition, the direction of SP can be also aligned to x or y axes, discussed later.

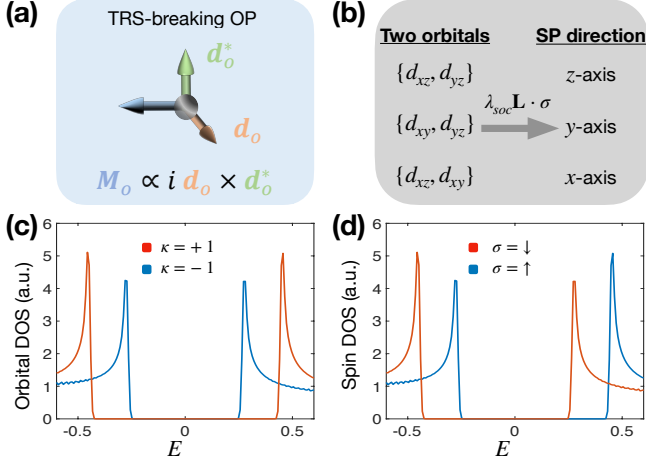


FIG. 5. (a) Schematic diagram showing the TRB orbital polarization (OP) induced by complex \mathbf{d}_o -vector. (b) Spin could be polarized in different directions based on the two active orbitals involved in the pairing. (c) Orbital DOS projected into the chiral $\kappa = \pm 1$ basis, showing a two-gap feature due to TRB. (d) The corresponding spin DOS, shifted relative to the fermi level due to the non-zero effective Zeeman field from the OP. Parameters used: $t_0 = 1, \mu = -2, \lambda_R = 0, \lambda_{soc} = 0.2, \Delta_o = 0.4, \lambda_o = 0, \mathbf{d}_o = (1, 0, e^{i\pi/10})$.

To verify the above analysis, we numerically solve the BdG Hamiltonian (6), $\mathcal{H}_{BdG}|E_n(\mathbf{k})\rangle = E_n(\mathbf{k})|E_n(\mathbf{k})\rangle$, where the n -th eigenstate is given by $|E_n(\mathbf{k})\rangle = (u_{d_{xz},\uparrow}^n, u_{d_{xz},\downarrow}^n, v_{d_{xz},\uparrow}^n, v_{d_{xz},\downarrow}^n, u_{d_{yz},\uparrow}^n, u_{d_{yz},\downarrow}^n, v_{d_{yz},\uparrow}^n, v_{d_{yz},\downarrow}^n)^T$. Thus, the atomic-orbital and spin-resolved DOS can be calculated as the following,

$$D_{orbit}^\kappa(E) = \sum_{\sigma, n, \mathbf{k}} |u_{\kappa, \sigma}^n|^2 \delta(E - E_n(\mathbf{k})),$$

$$D_{spin}^\sigma(E) = \sum_{\tau, n, \mathbf{k}} |u_{\tau, \sigma}^n|^2 \delta(E - E_n(\mathbf{k})),$$
(38)

where $u_{\kappa, \sigma}^n = \frac{1}{\sqrt{2}}(u_{d_{xz}, \sigma}^n - i\kappa u_{d_{yz}, \sigma}^n)$ and $\kappa = \pm 1$ for $d_{xz} \pm id_{yz}$ orbitals. In Fig. 5(c), $D_{orbit}^{+1} \neq D_{orbit}^{-1}$ indicates that the DOS is orbital-polarized. Remarkably, we also have $D_{spin}^\uparrow \neq D_{spin}^\downarrow$ due to coupling between electron spin and atomic orbitals, shown in Fig. 5(d). The difference in orbital DOS acts as an effective Zeeman field for the electron spins, hence shifts the spin DOS relative to the fermi level in opposite directions for up spin and down spin. This interesting phenomenon is quite different from spin-triplet SCs. In TRB spin-triplet SCs, The spin up channel and spin down channel will form different symmetric gaps in spin DOS, similar to the two orbital channels in Fig. 5(c) for our case. Therefore, the spin DOS profiles are distinct in the two cases. As a result, the spin-resolved DOS, which can be probed by spin-resolved STM [74], can serve as smoking gun evidence to identify TRB due to complex orbital \mathbf{d}_o -vector in multi-orbital SCs.

VI. DISCUSSIONS AND CONCLUSIONS

In the end, we briefly discuss the direction of spin-polarization induced by atomic orbital-polarization. We consider the three-dimensional subspace of t_{2g} orbitals spanned by $\{d_{yz}, d_{xz}, d_{xy}\}$, the matrix form of the angular momentum operators \mathbf{L} reads [55],

$$L_x = \begin{pmatrix} 0 & 0 & 0 \\ 0 & 0 & i \\ 0 & -i & 0 \end{pmatrix}, L_y = \begin{pmatrix} 0 & 0 & -i \\ 0 & 0 & 0 \\ i & 0 & 0 \end{pmatrix}, L_z = \begin{pmatrix} 0 & i & 0 \\ -i & 0 & 0 \\ 0 & 0 & 0 \end{pmatrix},$$
(39)

which satisfy the commutation relation $[L_m, L_n] = -i\epsilon_{mnl}L_l$. Therefore, the spin-orbit coupling for a system with the t_{2g} orbitals is given by,

$$H_{soc} = \lambda_{soc} \mathbf{L} \cdot \boldsymbol{\sigma}. \quad (40)$$

Then, let us consider a two-orbital system, the above SOC Hamiltonian will be reduced to,

$$\begin{cases} \text{For } \{d_{yz}, d_{xz}\}: H_{soc} = -\lambda_{soc}\tau_2\sigma_3, \\ \text{For } \{d_{yz}, d_{xy}\}: H_{soc} = \lambda_{soc}\tau_2\sigma_2, \\ \text{For } \{d_{xz}, d_{xy}\}: H_{soc} = -\lambda_{soc}\tau_2\sigma_1. \end{cases} \quad (41)$$

Therefore, in the above three cases, the spin-polarization is pointed to z, y, x -axis, respectively. Because the atomic orbital polarization is induced by the complex orbital \mathbf{d}_o -vector as $(0, M_o^y, 0) \propto i\mathbf{d}_o^* \times \mathbf{d}_o$.

To summarize, we establish a phenomenological theory for spin-singlet two-band SCs and discuss the distinct features of both TRI non-unitary pairings and TRB non-unitary pairings. Practically, we demonstrate that the stability of orbital-dependent pairing states could give birth to the non-unitary pairing states in a purely spin-singlet SC. Remarkably, the interplay between atomic SOC and orbital-dependent pairings is also investigated and we find a new spin-orbit-coupled SC with spin-singlet non-unitary pairing. For this exotic state, there are mainly three features. Firstly, the atomic SOC could enlarge the in-plane upper critical field compared to the Pauli limit. Secondly, topological chiral or helical superconductivity could be realized even in the absence of external magnetic fields or Zeeman fields. Furthermore, a spontaneous TRB SC could even generate a spin-polarized superconducting state that can be detected by measuring the spin-resolved density of states. We hope our theory leads to a deeper understanding of spin-singlet non-unitary SCs.

Our theory might have potential applications to the intriguing Sr_2SuO_4 [75, 76], LaNiGa_2 [50], iron-based SCs [51, 52] and ultra-cold atomic systems with large spin alkali and alkaline-earth fermions [77–81].

VII. ACKNOWLEDGMENTS

We thank J.-L. Lado, R.-X. Zhang and C.-X. Liu for helpful discussions. We especially acknowledge J.-

L. Lado's careful reading of the manuscript. D.-H.X. was supported by the NSFC (under Grant Nos. 12074108 and 11704106).

Appendix A: Derivation of T_c from linearized gap equation

Starting from the generic Hamiltonian, containing atomic SOC, orbital hybridization and in-plane magnetic field,

$$H_0(\mathbf{k}) = \epsilon(\mathbf{k}) + \lambda_{soc}\sigma_3\tau_2 + \lambda_o(g_1\tau_1 + g_3\tau_3) + h\sigma_1. \quad (\text{A1})$$

The Matsubara Green's function for electrons is

$$\begin{aligned} G_e(\mathbf{k}, i\omega_n) &= [i\omega_n - \mathcal{H}_0(\mathbf{k})]^{-1} \\ &= \frac{P_{---}}{i\omega_n - \epsilon_{\mathbf{k}} + E_-} + \frac{P_{++-}}{i\omega_n - \epsilon_{\mathbf{k}} + E_+} + \frac{P_{-+-}}{i\omega_n - \epsilon_{\mathbf{k}} - E_-} + \frac{P_{+++}}{i\omega_n - \epsilon_{\mathbf{k}} - E_+}, \end{aligned} \quad (\text{A2})$$

where the projection operator

$$P_{\alpha\beta\gamma} = \frac{1}{4}[1 + \alpha(g_1\sigma_1\tau_1 + g_3\sigma_1\tau_3)] \cdot [1 + \frac{\beta}{E_\gamma}(\lambda_{soc}\sigma_3\tau_2 + \lambda_o(g_1\tau_1 + g_3\tau_3) + h\sigma_1)], \quad (\text{A3})$$

with $\alpha, \beta, \gamma \in \{+, -\}$ and $E_\gamma = \sqrt{\lambda_{soc}^2 + (\lambda_o + \gamma h)^2}$. The Green's function for hole is $G_h(\mathbf{k}, i\omega_n) = -G_e^*(\mathbf{k}, i\omega_n)$. Here $\omega_n = (2n + 1)\pi k_B T$.

The linearized gap equation is given by

$$\Delta_{s_1, s_2}^{a, b}(\mathbf{k}) = -\frac{1}{\beta} \sum_{\omega_n} \sum_{s'_1 a', s'_2 b'} V_{s'_1 a', s'_2 b'}^{s_1 a, s_2 b}(\mathbf{k}, \mathbf{k}') \times \left[G_e(\mathbf{k}', i\omega_n) \hat{\Delta}(\mathbf{k}') G_h(-\mathbf{k}', i\omega_n) \right]_{s'_1 a', s'_2 b'}, \quad (\text{A4})$$

where the generic attractive interaction can be expanded as

$$V_{s'_1 a', s'_2 b'}^{s_1 a, s_2 b}(\mathbf{k}, \mathbf{k}') = -v_0 \sum_{\Gamma, m} [\mathbf{d}_o^{\Gamma, m}(\mathbf{k}) \cdot \boldsymbol{\tau} i\sigma_2]_{s_1 a, s_2 b} [\mathbf{d}_o^{\Gamma, m}(\mathbf{k}') \cdot \boldsymbol{\tau} i\sigma_2]_{s'_1 a', s'_2 b'}, \quad (\text{A5})$$

where $v_0 > 0$ and Γ labels the irreducible representation with m -dimension of crystalline groups. The linearized gap equation is reduced to $v_0 \chi(T) - 1 = 0$ where $\chi(T)$ is the superconductivity susceptibility.

For orbital-independent pairing:

$$\chi(T)_s = -\frac{1}{\beta} \sum_{\mathbf{k}, \omega_n} \text{Tr} [(\psi_s(\mathbf{k}) i\sigma_2)^\dagger G_e(\mathbf{k}, i\omega_n) (\psi_s(\mathbf{k}) i\sigma_2) G_h(-\mathbf{k}, i\omega_n)]. \quad (\text{A6})$$

For orbital-dependent pairing:

$$\chi(T)_o = -\frac{1}{\beta} \sum_{\mathbf{k}, \omega_n} \text{Tr} [(\mathbf{d}_o(\mathbf{k}) \cdot \boldsymbol{\tau} i\sigma_2)^\dagger G_e(\mathbf{k}, i\omega_n) (\mathbf{d}_o(\mathbf{k}) \cdot \boldsymbol{\tau} i\sigma_2) G_h(-\mathbf{k}, i\omega_n)]. \quad (\text{A7})$$

Then we take the standard replacement, $\sum_{\mathbf{k}, \omega_n} \rightarrow \frac{N_0}{4} \int_{-\omega_D}^{+\omega_D} d\epsilon \int_S d\Omega \sum_{\omega_n}$, where N_0 is the density of states at Fermi surface, Ω is the solid angle of \mathbf{k} on Fermi surfaces and ω_D the Deybe frequency. We will also be making use of,

$$-\frac{N_0}{\beta} \int_{-\omega_D}^{+\omega_D} \sum_{\omega_n} d\epsilon G_e^+(\mathbf{k}, i\omega_n) G_h^+(\mathbf{k}, i\omega_n) = -\frac{N_0}{\beta} \int_{-\omega_D}^{+\omega_D} \sum_{\omega_n} G_e^-(\mathbf{k}, i\omega_n) G_h^-(\mathbf{k}, i\omega_n) = \chi_0(T), \quad (\text{A8})$$

$$-\frac{N_0}{\beta} \int_{-\omega_D}^{+\omega_D} \sum_{\omega_n} d\epsilon G_e^-(\mathbf{k}, i\omega_n) G_h^+(\mathbf{k}, i\omega_n) = -\frac{N_0}{\beta} \int_{-\omega_D}^{+\omega_D} \sum_{\omega_n} G_e^+(\mathbf{k}, i\omega_n) G_h^-(\mathbf{k}, i\omega_n) = \chi_0(T) + N_0 \mathcal{C}_0(T), \quad (\text{A9})$$

where $\chi_0(T) = N_0 \ln \left(\frac{2e^{\gamma} \omega_D}{\pi k_B T} \right)$, $\gamma = 0.57721 \dots$ the Euler-Mascheroni constant and $\mathcal{C}_0(T) = \text{Re}[\psi^{(0)}(\frac{1}{2}) - \psi^{(0)}(\frac{1}{2} + i \frac{E(\mathbf{k})}{2\pi k_B T})]$ with $\psi^{(0)}(z)$ being the digamma function.

For orbital-independent pairing considered in the main text $\Delta_s \tau_0 i \sigma_2$, we have

$$\begin{aligned} \chi_s(T) &= \chi_0(T) + \frac{N_0}{2} \left[\mathcal{C}_0 \left(T, \frac{E_+ - E_-}{2} \right) + \mathcal{C}_0 \left(T, \frac{E_+ + E_-}{2} \right) \right] \\ &\quad + \frac{N_0}{2} \left[\mathcal{C}_0 \left(T, \frac{E_+ - E_-}{2} \right) - \mathcal{C}_0 \left(T, \frac{E_+ + E_-}{2} \right) \right] \times \frac{\lambda_o^2 + \lambda_{soc}^2 - h^2}{E_+ E_-} \\ &\equiv \chi_0(T) + N_0 f_s(T, \lambda_{soc}, \lambda_o, h). \end{aligned} \quad (\text{A10})$$

In order to look at the effect of λ_o on the Pauli limit, we could Taylor expand $f_s(T, \lambda_{soc}, \lambda_o, h)$ for small λ_o :

$$f_s(T, \lambda_{soc}, \lambda_o, h) = f_s(T, \lambda_{soc}, 0, h) + F(T, \lambda_{soc}, h) \lambda_o^2 + \mathcal{O}(\lambda_o^4), \quad (\text{A11})$$

with

$$\begin{aligned} F(T, \lambda_{soc}, h) &= \psi^{(2)}(\frac{1}{2}) \frac{\lambda_{soc}^2 h^2}{4\pi k_B^2 T^2 (\lambda_{soc}^2 + h^2)^2} \\ &\quad - \text{Re}\{\psi^{(0)}(\frac{1}{2}) - \psi^{(0)}(\frac{1}{2} + i \frac{\sqrt{\lambda_{soc}^2 + h^2}}{2\pi k_B T})\} \frac{4\lambda_{soc}^2 h^2}{(\lambda_{soc}^2 + h^2)^3} \\ &\quad + \text{Im}\{\psi^{(1)}(\frac{1}{2} + i \frac{\sqrt{\lambda_{soc}^2 + h^2}}{2\pi k_B T})\} \frac{\lambda_{soc}^2 h^2}{2\pi k_B T (\lambda_{soc}^2 + h^2)^{5/2}}. \end{aligned} \quad (\text{A12})$$

This is used in the main text.

For orbital-dependent pairing $\Delta_o(d_1 \tau_1 + d_3 \tau_3) i \sigma_2$ with $\mathbf{d}_o = \mathbf{g}_o$, we have

$$\begin{aligned} \chi_o(T) &= \chi_0(T) + \frac{N_0}{2} \left[\mathcal{C}_0 \left(T, \frac{E_+ - E_-}{2} \right) + \mathcal{C}_0 \left(T, \frac{E_+ + E_-}{2} \right) \right] \\ &\quad + \frac{N_0}{2} \left[\mathcal{C}_0 \left(T, \frac{E_+ - E_-}{2} \right) - \mathcal{C}_0 \left(T, \frac{E_+ + E_-}{2} \right) \right] \times \frac{\lambda_o^2 - \lambda_{soc}^2 - h^2}{E_+ E_-} \\ &\equiv \chi_0(T) + N_0 f_o(T, \lambda_{soc}, \lambda_o, h). \end{aligned} \quad (\text{A13})$$

Appendix B: TSC with $\Delta_s = 0, \lambda_o = 0$

To demonstrate the topology, we also show a simple case with $\Delta_s = 0$ and $\lambda_o = 0$, where the Z_2 can be characterized analytically.

In this section we focus on the simplified case without orbital independent pairing or orbital hybridization. In Fig. ??(a), we calculate the edge spectrum with k_x being a good quantum number in a semi-infinite geometry, and it shows the corresponding bulk band structure together with two counter-propagating MEMs. The bulk topology of the 2D helical TSC phase is characterized by the Z_2 topological invariant ν , which can be extracted by calculating the Wilson-loop spectrum. And, $\nu = 1 \pmod{2}$ characterizes the helical TSC. In Fig. 2(b), we plot the evolution of θ as a function of k_y , and the winding pattern indicates the topological Z_2 invariant $\nu = 1$.

On the other hand, with $\Delta_s = 0$, which is the case if we only consider on-site attractive interactions between electrons [82, 83], the BdG Hamiltonian (6) can be decomposed into two orbital subspaces that are related through time-reversal transformation. Each of these blocks has

a well-defined Chern number because each block alone breaks TRS. The two Chern numbers can then be used to define the Z_2 invariant of the whole BdG system. The detailed procedures are the following.

For the normal Hamiltonian given in Eq. (3), we have $[\mathcal{H}_0, \tau_2] = 0$. As a result, we can project the normal Hamiltonian \mathcal{H}_0 in Eq. (3) into block-diagonal form corresponding to the ± 1 eigenvalues of τ_2 by using the basis transformation $\mathcal{U} = \sigma_0 \otimes \frac{1}{\sqrt{2}} \begin{bmatrix} 1 & -i \\ 1 & i \end{bmatrix}$. The new basis is given by

$$\tilde{\Psi}^\dagger(\mathbf{k}) = (c_{+, \uparrow}^\dagger, c_{+, \downarrow}^\dagger, c_{-, \downarrow}^\dagger, c_{-, \uparrow}^\dagger), \quad (\text{B1})$$

where $c_{\pm, s}^\dagger \equiv \frac{1}{\sqrt{2}}(c_{d_{xz}, s}^\dagger \mp i c_{d_{yz}, s}^\dagger)$. In this basis the normal Hamiltonian is given by

$$\mathcal{H}_0 = \mathcal{H}_0^+ \oplus \mathcal{H}_0^-, \quad (\text{B2})$$

where \mathcal{H}_0^\pm are given by

$$\mathcal{H}_0^\pm = \epsilon(\mathbf{k}) + \lambda_R(k_x \sigma_2 - k_y \sigma_1) \mp \lambda_{soc} \sigma_3. \quad (\text{B3})$$

Note that the time-reversal transforms $\mathcal{H}_0^\pm(\mathbf{k})$ to $\mathcal{H}_0^\mp(-\mathbf{k})$. In the new basis the pairing Hamiltonian also decouples as $\mathcal{H}_\Delta = \mathcal{H}_\Delta^+ \oplus \mathcal{H}_\Delta^-$ with \mathcal{H}_Δ^\pm given by

$$\mathcal{H}_\Delta^\pm = 2\Delta_\pm \left[c_{\pm,\uparrow}^\dagger(\mathbf{k})c_{\pm,\downarrow}^\dagger(-\mathbf{k}) - (\uparrow \leftrightarrow \downarrow) \right] + \text{h.c.}, \quad (\text{B4})$$

where $\Delta_\pm \equiv \Delta_o(\mp id_o^1 + d_o^3)$ are the gap strengths in each subspace. Therefore, the Bogoliubov de-Gennes (BDG) Hamiltonian takes the following block-diagonal form,

$$\mathcal{H}_{BdG} = \mathcal{H}_{BdG}^+ \oplus \mathcal{H}_{BdG}^-, \quad (\text{B5})$$

where

$$\mathcal{H}_{BdG}^\pm(\mathbf{k}) = (\epsilon(\mathbf{k}) \mp \lambda_{soc}\sigma_3)\gamma_3 + \lambda_R(k_x\sigma_2\gamma_3 - k_y\sigma_1\gamma_0) \pm 2d_1\sigma_2\gamma_1 - 2d_3\sigma_2\gamma_2, \quad (\text{B6})$$

with γ_μ being the Pauli matrices in the particle-hole space. The Nambu basis is $\Psi_\pm^\dagger(\mathbf{k}) = (c_{\pm,\uparrow}^\dagger(\mathbf{k}), c_{\pm,\downarrow}^\dagger(\mathbf{k}), c_{\pm,\uparrow}(-\mathbf{k}), c_{\pm,\downarrow}(-\mathbf{k}))$. Each subspace has its own particle-hole symmetry.

By symmetry, the 2D BdG Hamiltonian in Eq. (B5) belongs to Class DIII of the A-Z classification[84, 85] for topological insulators and superconductors because both TRS and particle-hole symmetry are preserved. However, it is not the case for our model. The BdG Hamiltonian here could exhibit topological states with Z_2 type topological invariant, which can be defined as the following. In each subspace, we define the BdG Chern number as

$$\mathcal{C}_\pm = \frac{1}{2\pi} \sum_{\text{filled bands}} \int_{BZ} d\mathbf{k} \cdot \langle \phi_n^\pm(\mathbf{k}) | i\nabla_{\mathbf{k}} | \phi_n^\pm(\mathbf{k}) \rangle, \quad (\text{B7})$$

with $|\phi_n^\pm\rangle$ being the energy eigenstate of \mathcal{H}_{BdG}^\pm . Then the Z_2 invariant in this case is then explicitly given by,

$$\nu \equiv \frac{\mathcal{C}_+ - \mathcal{C}_-}{2}, \quad (\text{B8})$$

where \mathcal{C}_\pm are the Chern numbers of the \pm channels. Fig. 3(c) shows the change in ν when the chemical potential μ is tuned, which is consistent with the Wilson-loop calculation shown in Fig. 3(b). Fig. 3(d) is the corresponding schematic phase diagram.

Appendix C: Wilson loop calculation for Z_2 TSC

In the thermodynamics limit, the Wilson loop operator along a closed path p is expressed as

$$\mathcal{W}_p = \mathcal{P} \exp \left[i \oint_p \mathcal{A}(\mathbf{k}) d\mathbf{k} \right], \quad (\text{C1})$$

where \mathcal{P} means path ordering and $\mathcal{A}(\mathbf{k})$ is the non-Abelian Berry connection

$$\mathcal{A}^{nm}(\mathbf{k}) = i \langle \phi^n(\mathbf{k}) | \nabla_{\mathbf{k}} | \phi^m(\mathbf{k}) \rangle, \quad (\text{C2})$$

with $|\phi^{m,n}(\mathbf{k})\rangle$ the occupied eigenstates. The Wilson line element is defined as

$$G^{mm}(\mathbf{k}) = \langle \phi^n(\mathbf{k} + \Delta\mathbf{k}) | \phi^m(\mathbf{k}) \rangle, \quad (\text{C3})$$

where the $\mathbf{k} = (k_x, k_y)$, and $\Delta\mathbf{k} = (0, 2\pi/N_y)$ is the steps. In the discrete case, the Wilson loop operator on a path along k_y from the initial point \mathbf{k} to the final point $\mathbf{k} + (0, 2\pi)$ can be written as $\mathcal{W}_{y,\mathbf{k}} = G(\mathbf{k} + (N_y - 1)\Delta\mathbf{k})G(\mathbf{k} + (N_y - 2)\Delta\mathbf{k}) \dots G(\mathbf{k} + \Delta\mathbf{k})G(\mathbf{k})$, which satisfies the eigenvalue equation

$$\mathcal{W}_{y,\mathbf{k}} |\nu_{y,\mathbf{k}}^j\rangle = e^{i2\pi\nu_y^j(k_x)} |\nu_{y,\mathbf{k}}^j\rangle \quad (\text{C4})$$

The phase of eigenvalue $\theta = 2\pi\nu_y^j(k_x)$ is the Wannier function center.

-
- [1] M. Sigrist and K. Ueda, Rev. Mod. Phys. **63**, 239 (1991).
[2] V. P. Mineev, K. Samokhin, and L. Landau, *Introduction to unconventional superconductivity* (CRC Press, 1999).
[3] F. Steglich, J. Aarts, C. D. Bredl, W. Lieke, D. Meschede, W. Franz, and H. Schäfer, Phys. Rev. Lett. **43**, 1892 (1979).
[4] J. G. Bednorz and K. A. Müller, Z. Physik B - Condensed Matter **64**, 189 (1986).
[5] F. C. Zhang and T. M. Rice, Phys. Rev. B **37**, 3759 (1988).
[6] P. W. Anderson, P. Lee, M. Randeria, T. Rice, N. Trivedi, and F. Zhang, Journal of Physics: Condensed Matter **16**, R755 (2004).
[7] D. J. Scalapino, Rev. Mod. Phys. **84**, 1383 (2012).
[8] P. M. R. Brydon, D. S. L. Abergel, D. F. Agterberg, and V. M. Yakovenko, Phys. Rev. X **9**, 031025 (2019).
[9] T. M. R. Wolf, M. F. Holst, M. Sigrist, and J. L. Lado, arXiv e-prints, arXiv:2108.01452 (2021), arXiv:2108.01452 [cond-mat.mes-hall].
[10] M. Zeng, D.-H. Xu, Z.-M. Wang, L.-H. Hu, and F.-C. Zhang, arXiv e-prints, arXiv:2109.06039 (2021), arXiv:2109.06039 [cond-mat.supr-con].
[11] X. Dai, Z. Fang, Y. Zhou, and F.-C. Zhang, Phys. Rev. Lett. **101**, 057008 (2008).
[12] T. T. Ong and P. Coleman, Phys. Rev. Lett. **111**, 217003 (2013).
[13] Z. P. Yin, K. Haule, and G. Kotliar, Nature Physics **10**, 845 (2014).
[14] T. Ong, P. Coleman, and J. Schmalian, Proceedings of the National Academy of Sciences **113**, 5486 (2016).
[15] R. Nourafkan, G. Kotliar, and A.-M. S. Tremblay, Phys. Rev. Lett. **117**, 137001 (2016).

- [16] A. V. Chubukov, O. Vafek, and R. M. Fernandes, *Phys. Rev. B* **94**, 174518 (2016).
- [17] M. Yi, Y. Zhang, Z.-X. Shen, and D. Lu, *npj Quantum Materials* **2**, 1 (2017).
- [18] E. M. Nica, R. Yu, and Q. Si, *npj Quantum Materials* **2**, 1 (2017).
- [19] P. O. Sprau, A. Kostin, A. Kreisel, A. E. Böhrer, V. Taufour, P. C. Canfield, S. Mukherjee, P. J. Hirschfeld, B. M. Andersen, and J. S. Davis, *Science* **357**, 75 (2017).
- [20] H. Hu, R. Yu, E. M. Nica, J.-X. Zhu, and Q. Si, *Phys. Rev. B* **98**, 220503 (2018).
- [21] E. M. Nica and Q. Si, *npj Quantum Materials* **6**, 1 (2021).
- [22] L. A. Wray, S.-Y. Xu, Y. Xia, Y. San Hor, D. Qian, A. V. Fedorov, H. Lin, A. Bansil, R. J. Cava, and M. Z. Hasan, *Nature Physics* **6**, 855 (2010).
- [23] L. Fu and E. Berg, *Phys. Rev. Lett.* **105**, 097001 (2010).
- [24] P. M. R. Brydon, L. Wang, M. Weinert, and D. F. Agterberg, *Phys. Rev. Lett.* **116**, 177001 (2016).
- [25] W. Yang, Y. Li, and C. Wu, *Phys. Rev. Lett.* **117**, 075301 (2016).
- [26] D. F. Agterberg, P. M. R. Brydon, and C. Timm, *Phys. Rev. Lett.* **118**, 127001 (2017).
- [27] L. Savary, J. Ruhman, J. W. F. Venderbos, L. Fu, and P. A. Lee, *Phys. Rev. B* **96**, 214514 (2017).
- [28] W. Yang, T. Xiang, and C. Wu, *Phys. Rev. B* **96**, 144514 (2017).
- [29] C. Timm, A. P. Schnyder, D. F. Agterberg, and P. M. R. Brydon, *Phys. Rev. B* **96**, 094526 (2017).
- [30] J. Yu and C.-X. Liu, *Phys. Rev. B* **98**, 104514 (2018).
- [31] I. Boettcher and I. F. Herbut, *Phys. Rev. Lett.* **120**, 057002 (2018).
- [32] B. Roy, S. A. A. Ghorashi, M. S. Foster, and A. H. Nevidomskyy, *Phys. Rev. B* **99**, 054505 (2019).
- [33] H. Kim, K. Wang, Y. Nakajima, R. Hu, S. Ziemak, P. Syers, L. Wang, H. Hodovanets, J. D. Denlinger, P. M. Brydon, *et al.*, *Science advances* **4**, eaao4513 (2018).
- [34] D. F. Agterberg, T. M. Rice, and M. Sigrist, *Phys. Rev. Lett.* **78**, 3374 (1997).
- [35] T. Takimoto, *Phys. Rev. B* **62**, R14641 (2000).
- [36] W. Huang, Y. Zhou, and H. Yao, *Phys. Rev. B* **100**, 134506 (2019).
- [37] Z.-M. Wang, M. Zeng, C. Lu, L.-H. Hu, and D.-H. Xu, *In preparation* (2022).
- [38] W. Yang, C. Xu, and C. Wu, *Phys. Rev. Research* **2**, 042047 (2020).
- [39] N. F. Q. Yuan, W.-Y. He, and K. T. Law, *Phys. Rev. B* **95**, 201109 (2017).
- [40] L. Chirolli, F. de Juan, and F. Guinea, *Phys. Rev. B* **95**, 201110 (2017).
- [41] A. Robins and P. Brydon, *Journal of Physics: Condensed Matter* **30**, 405602 (2018).
- [42] J. L. Lado and M. Sigrist, *Phys. Rev. Research* **1**, 033107 (2019).
- [43] L.-H. Hu, P. D. Johnson, and C. Wu, *Phys. Rev. Research* **2**, 022021 (2020).
- [44] Y. Saito, Y. Nakamura, M. S. Bahramy, Y. Kohama, J. Ye, Y. Kasahara, Y. Nakagawa, M. Onga, M. Tokunaga, T. Nojima, *et al.*, *Nature Physics* **12**, 144 (2016).
- [45] J. Lu, O. Zheliuk, I. Leermakers, N. F. Yuan, U. Zeitler, K. T. Law, and J. Ye, *Science* **350**, 1353 (2015).
- [46] X. Xi, Z. Wang, W. Zhao, J.-H. Park, K. T. Law, H. Berger, L. Forró, J. Shan, and K. F. Mak, *Nature Physics* **12**, 139 (2016).
- [47] J. Falson, Y. Xu, M. Liao, Y. Zang, K. Zhu, C. Wang, Z. Zhang, H. Liu, W. Duan, K. He, *et al.*, *Science* **367**, 1454 (2020).
- [48] A. D. Hillier, J. Quintanilla, and R. Cywinski, *Phys. Rev. Lett.* **102**, 117007 (2009).
- [49] A. D. Hillier, J. Quintanilla, B. Mazidian, J. F. Annett, and R. Cywinski, *Phys. Rev. Lett.* **109**, 097001 (2012).
- [50] Z. F. Weng, J. L. Zhang, M. Smidman, T. Shang, J. Quintanilla, J. F. Annett, M. Nicklas, G. M. Pang, L. Jiao, W. B. Jiang, Y. Chen, F. Steglich, and H. Q. Yuan, *Phys. Rev. Lett.* **117**, 027001 (2016).
- [51] V. Grinenko, R. Sarkar, K. Kihou, C. Lee, I. Morozov, S. Aswartham, B. Büchner, P. Chekhonin, W. Skrotzki, K. Nenkov, *et al.*, *Nature Physics* , 1 (2020).
- [52] N. Zaki, G. Gu, A. Tsvetik, C. Wu, and P. D. Johnson, *Proceedings of the National Academy of Sciences* **118** (2021).
- [53] P. K. Biswas, S. K. Ghosh, J. Z. Zhao, D. A. Mayoh, N. D. Zhigadlo, X. Xu, C. Baines, A. D. Hillier, G. Balakrishnan, and M. R. Lees, *Nature communications* **12**, 2504 (2021).
- [54] L.-H. Hu, X. Wang, and T. Shang, *Phys. Rev. B* **104**, 054520 (2021).
- [55] W.-C. Lee, D. P. Arovas, and C. Wu, *Phys. Rev. B* **81**, 184403 (2010).
- [56] Y. Wang and L. Fu, *Phys. Rev. Lett.* **119**, 187003 (2017).
- [57] C. Wang, B. Lian, X. Guo, J. Mao, Z. Zhang, D. Zhang, B.-L. Gu, Y. Xu, and W. Duan, *Phys. Rev. Lett.* **123**, 126402 (2019).
- [58] X.-L. Qi, T. L. Hughes, S. Raghu, and S.-C. Zhang, *Phys. Rev. Lett.* **102**, 187001 (2009).
- [59] C.-X. Liu and B. Trauzettel, *Phys. Rev. B* **83**, 220510 (2011).
- [60] S. Nakosai, Y. Tanaka, and N. Nagaosa, *Phys. Rev. Lett.* **108**, 147003 (2012).
- [61] S. Deng, L. Viola, and G. Ortiz, *Phys. Rev. Lett.* **108**, 036803 (2012).
- [62] F. Zhang, C. L. Kane, and E. J. Mele, *Phys. Rev. Lett.* **111**, 056402 (2013).
- [63] J. Wang, Y. Xu, and S.-C. Zhang, *Phys. Rev. B* **90**, 054503 (2014).
- [64] A. Haim and Y. Oreg, *Physics Reports* **825**, 1 (2019).
- [65] O. E. Casas, L. Arrachea, W. J. Herrera, and A. L. Yeyati, *Phys. Rev. B* **99**, 161301 (2019).
- [66] Y. Volpez, D. Loss, and J. Klinovaja, *Phys. Rev. Research* **2**, 023415 (2020).
- [67] R.-X. Zhang and S. Das Sarma, *Phys. Rev. Lett.* **126**, 137001 (2021).
- [68] J.-F. Ge, Z.-L. Liu, C. Liu, C.-L. Gao, D. Qian, Q.-K. Xue, Y. Liu, and J.-F. Jia, *Nature Materials* **14**, 285 (2014).
- [69] R. Yu, X. L. Qi, A. Bernevig, Z. Fang, and X. Dai, *Phys. Rev. B* **84**, 075119 (2011).
- [70] W. A. Benalcazar, B. A. Bernevig, and T. L. Hughes, *Phys. Rev. B* **96**, 245115 (2017).
- [71] X.-L. Qi, T. L. Hughes, and S.-C. Zhang, *Phys. Rev. B* **82**, 184516 (2010).
- [72] J. D. Sau, R. M. Lutchyn, S. Tewari, and S. Das Sarma, *Phys. Rev. Lett.* **104**, 040502 (2010).
- [73] T. Meng and L. Balents, *Phys. Rev. B* **86**, 054504 (2012).
- [74] R. Wiesendanger, *Reviews of Modern Physics* **81**, 1495 (2009).
- [75] G. M. Luke, Y. Fudamoto, K. Kojima, M. Larkin, J. Merriam, B. Nachumi, Y. Uemura, Y. Maeno, Z. Mao, Y. Mori,

- et al.*, Nature **394**, 558 (1998).
- [76] J. Xia, Y. Maeno, P. T. Beyersdorf, M. M. Fejer, and A. Kapitulnik, Phys. Rev. Lett. **97**, 167002 (2006).
- [77] T.-L. Ho and S. Yip, Phys. Rev. Lett. **82**, 247 (1999).
- [78] C. Wu, J.-p. Hu, and S.-c. Zhang, Phys. Rev. Lett. **91**, 186402 (2003).
- [79] B. J. DeSalvo, M. Yan, P. G. Mickelson, Y. N. Martinez de Escobar, and T. C. Killian, Phys. Rev. Lett. **105**, 030402 (2010).
- [80] S. Taie, Y. Takasu, S. Sugawa, R. Yamazaki, T. Tsujimoto, R. Murakami, and Y. Takahashi, Phys. Rev. Lett. **105**, 190401 (2010).
- [81] A. V. Gorshkov, M. Hermele, V. Gurarie, C. Xu, P. S. Julienne, J. Ye, P. Zoller, E. Demler, M. D. Lukin, and A. Rey, Nature physics **6**, 289 (2010).
- [82] C.-X. Liu, Phys. Rev. Lett. **118**, 087001 (2017).
- [83] L.-H. Hu, C.-X. Liu, and F.-C. Zhang, Communications Physics **2**, 1 (2019).
- [84] S. Ryu, A. P. Schnyder, A. Furusaki, and A. W. Ludwig, New Journal of Physics **12**, 065010 (2010).
- [85] C.-K. Chiu, J. C. Y. Teo, A. P. Schnyder, and S. Ryu, Rev. Mod. Phys. **88**, 035005 (2016).